



Finite Element Analysis of In-Service Loading on Hub Steering Knuckles: A Comparison of A356.0-T6 and Grey Cast Iron



Aniekan Essienubong Ikpe^{1*}, Jephthar Uviefowwe Ohwoekevw², Imoh Ime Ekanem²

¹ Department of Mechanical Engineering Technology, Akwa Ibom State Polytechnic, PMB. 1200 Ikot Osurua, Nigeria

² Department of Production Engineering, University of Benin, PMB. 1154 Benin City, Nigeria

* Correspondence: Aniekan Essienubong Ikpe (aniekan.ikpe@akwaibompoly.edu.ng)

Received: 12-18-2024

Revised: 02-06-2025

Accepted: 02-12-2025

Citation: A. E. Ikpe, J. U. Ohwoekevw, and I. I. Ekanem, "Finite element analysis of in-service loading on hub steering knuckles: A comparison of A356.0-T6 and grey cast iron," *Precis. Mech. Digit. Fabr.*, vol. 2, no. 1, pp. 12–30, 2025. <https://doi.org/10.56578/pmdf020102>.



© 2025 by the author(s). Licensee Acadlore Publishing Services Limited, Hong Kong. This article can be downloaded for free, and reused and quoted with a citation of the original published version, under the CC BY 4.0 license.

Abstract: This study investigates the structural response of a hub steering knuckle from a Toyota Camry LE under typical in-service loading conditions, with a focus on material performance comparison. Aluminium alloy A356.0-T6 and grey cast iron were selected as candidate materials for the analysis. A three-dimensional (3D) model of the hub steering knuckle was generated using SolidWorks 2018, while static structural simulations were conducted with ANSYS Workbench R15.0 (2019 version). The factor of safety (FOS) was varied between 2.293 and 15 to account for the diverse operational scenarios. The applied loading conditions were derived from the cumulative forces acting on the four tyres of the vehicle, with a total force of 3938.715 N in the Z-direction. The steering moment was calculated to be 5400 N·mm at a perpendicular distance of 108 mm, while the braking force amounted to 3964.63 N·mm, with a corresponding braking moment of 277,524.73 N·mm, all determined using standard analytical formulas. A solid mesh type was employed for the finite element analysis (FEA), with a blended curvature-based meshing technique applied. The results of the analysis showed that, for A356.0-T6, the maximum equivalent Von Mises stress (VMS), maximum equivalent elastic strain, maximum principal stress, and maximum shear stress were 36.079 MPa, 0.00018393 mm/mm, 44.587 MPa, and 19.871 MPa, respectively. In comparison, grey cast iron exhibited values of 24.016 MPa, 0.00013104 mm/mm, 41.214 MPa, and 18.625 MPa, respectively. The maximum directional deformations along the Z-axis for A356.0-T6 and grey cast iron were 0.010135 mm and 0.007275 mm, respectively. The maximum total deformations were recorded at 0.069036 mm and 0.048725 mm for A356.0-T6 and grey cast iron, respectively. These findings suggest that both materials are suitable for use in hub steering knuckles, with grey cast iron being preferable when impact resistance is a priority, whereas A356.0-T6 is more suitable for applications requiring lightweight and corrosion resistance. The results contribute to the understanding of material selection for automotive components, considering both mechanical performance and operational demands.

Keywords: Structural behaviour; Steering knuckle; Vehicle; Loading condition; Component deformation

1 Introduction

The hub steering knuckle is an essential element in the suspension system of a vehicle, responsible for connecting the wheel to the suspension system and allowing for steering movement. It plays a crucial role in supporting the weight of the vehicle, absorbing road shocks, and allowing for steering control. It serves as the point of convergence for the suspension and steering system, as well as the front wheels, enabling the steering mechanism to function autonomously [1, 2]. In addition, it functions as the intermediary component connecting the axle casing, stub axle, and tie rod. A kingpin serves as the linkage between the steering knuckle and the axle housing. On the opposite end, it connects to the tie rod. The knuckle fastens the wheel hub onto itself using a bearing. It also serves as the connection point where the upper and lower control arms, tie-rod ends, the spindle, as well as the wheels come together [3]. It enables vertical movement of the wheels when the suspension responds to uneven road surfaces and horizontal movement in response to steering commands. Therefore, the primary function of the steering knuckle is to convert the linear movement of the tie rod into the angular movement of the stub axle [4]. The structural behaviour of the hub steering knuckle is important for ensuring the stability and safety of the vehicle.

One of the factors that can significantly impact the structural behaviour of a hub steering knuckle configuration is the service load conditions experienced by the vehicle [5]. Vehicular loading conditions refer to the forces and stresses that are exerted on the vehicle components during normal operation. In-service loading conditions can vary depending on factors such as road conditions, driving habits, speed, and vehicle weight, which can have a significant impact on the structural behaviour of the hub steering knuckle [6]. Rough roads, potholes, and uneven surfaces can also subject the hub steering knuckle to high-impact loads, leading to stress concentrations, fatigue, and potential failure. In other words, the effect of vehicular in-service loading conditions on the structural behaviour of a hub steering knuckle configuration can be significant [7]. Excessive loading can lead to increased stress on the knuckle, potentially causing fatigue failure or deformation. This can result in reduced steering control, increased wear and tear on other suspension components, and ultimately compromise the safety and performance of the vehicle [8, 9]. Driving habits, such as aggressive driving, sudden braking, and sharp turns, can also increase the loading on the hub steering knuckle, further affecting its structural behaviour. The hub steering knuckle is subjected to various types of loading conditions during its service life, including static loads, dynamic loads, and impact loads. These loading conditions can cause stress concentrations, fatigue, and ultimately lead to failure of the hub steering knuckle [2, 10]. Vehicle weight is another important factor that influences the structural behaviour of the hub steering knuckle. Heavier vehicles exert higher loads on the hub steering knuckle, increasing the risk of stress concentrations and fatigue. Moreover, overloading the vehicle beyond its capacity can lead to premature failure of the hub steering knuckle. It is essential for manufacturers to consider in-service loading conditions when designing hub steering knuckles to ensure their structural integrity and performance [11, 12]. Proper material selection, design optimization, and testing under realistic loading conditions are crucial to ensure that the steering knuckle is able to withstand the forces and stresses it will encounter during operation and to withstand the demands of everyday driving while providing a safe and reliable driving experience for consumers. Despite being initially introduced in the 18th century, steering knuckles have experienced a significant surge in popularity since then. Automobiles, trucks, buses, and other sizable and weighty vehicles use these objects [13]. They link to the suspension system, facilitating the vehicle's smooth movement in various directions and aiding in steering.

The steering knuckle is a crucial element of the vehicle's suspension system, responsible for facilitating the rotation of the wheel [14]. The steering knuckles serve as the convergence point for the front wheels, suspension, and steering system. They provide attachment locations for the tie-rod ends, spindles, hubs, upper and lower control arms or struts, as well as other components that secure the wheels. The steering knuckles facilitate the wheels' ability to move in both horizontal and vertical directions in line with the steering input and the suspension's responsiveness to irregularities on the road [15]. There are a multitude of different variants of steering knuckles. They consist of a range of designs that fit different applications and types of suspension. However, they can be categorized into two distinct types: spindle and hub. The subject of this analysis is the steering knuckle from a Toyota Camry LE saloon vehicle. The car sector is increasingly concerned about reducing weight. Weight reduction can have a significant impact on emissions reduction (greenhouse gases), fuel economy improvement, and environmental protection. Various technological breakthroughs, such as improvements in materials, design and analytical procedures, production processes, and optimization techniques, have the potential to reduce weight. The steering knuckle experiences different loads over time during its operational lifespan, resulting in fatigue failure. Therefore, a crucial aspect of the component manufacturing is its design [16–19]. Furthermore, there is a growing focus in the automotive industry on enhancing the lifespan of car components that undergo unpredictable, non-proportional multi-input loading, specifically in terms of high-cycle fatigue (HCF). The road and various other components, including the joints between the knuckle and the lower control arm, steering linkage, and Macpherson strut, subject the steering knuckle to numerous unpredictable forces. Moreover, an incorrect adjustment of the wheel angle amplifies the magnitude of road strains. Previous studies have demonstrated that the wheel angles influence the service life of a component [20].

Yadav et al. [21] utilized forged steel EN 47 to develop and analyze a steering knuckle. The average weight of the vehicle included in their analysis was 1240 kg. The component was developed utilising Creo (Pro-E) 2.0 and subjected to static analysis via ANSYS Workbench 15.0. The observed maximum overall deformation was 0.89651 mm, whereas the highest lateral deformation along the X-axis was 0.62675 mm. The peak primary stress observed was 70.295 MPa, while the peak shear stress was recorded as 62.111 MPa. The maximum corresponding VMS recorded was 112.25, while the peak corresponding elastic strain measured was 0.00069023. The peak measured shear elastic strain was 0.00080745. Density of the material (7700 kg/m^3) and corrosion qualities were identified as potential drawbacks for its use in steering knuckle applications, in addition to its enhanced yield strength. A study was conducted using mild steel and a composite of mild steel with nickel. The study vehicle had an average weight of 1240 kg. The directional deformation at the X, Y, and Z axes was measured to be 0.392 mm, 0.21422 mm, and 0.3534 mm, respectively. The total deformation was found to be 1.8643 mm. The equivalent elastic strain was computed to be 0.026808, the maximum principal elastic strain to be 0.021241, and the equivalent VMS was determined to be 4467.6 MPa. Nevertheless, the bulk density of the materials posed a major challenge. Dusane et al. [22] performed an investigation on the steering knuckle of All Terrain Vehicles (ATV). The CAD model was

made with CATIA V5, and the frame of the steering knuckle, which is made of aluminum alloy 6061-T6, and the spindle, which is made of EN8 material, were analyzed using ANSYS 12. It was determined that Aluminum 6061-T6 alloy and EN8 are superior materials for steering knuckles due to their favourable physical and mechanical qualities, including their less dense nature. Both materials had a mass density of 2700 kg/m^3 , including a tensile yield strength of 276 MPa. Kashyzadeh [23] conducted a static analysis of composite steering knuckles, taking into account the road prerequisite defined by its roughness and contours. The vehicle model's driving state was simulated via multi-body dynamics (MBD) methodology. The stresses exerted on the linkages between the steering knuckle and other suspension components were determined, considering different car movements. Data was employed from a coordinate measuring machine (CMM) to create the steering knuckle model using CATIA software. According to the normal stress criterion, an increase in tungsten carbide content was directly correlated with an increase in the steering knuckle's robustness when subjected to solely axial loads. The shear stress criterion showed that as the amount of this material increased, the strength of the parts that were subjected to shear loads decreased. The study's circumstances determined that the use of metal matrix composites is not appropriate for this supercritical component.

This study aims to analyse the structural stability of a standard hub steering knuckle in a Toyota Camry LE saloon vehicle by considering the impact of in-service loads on the component's structural stability and performance. In this study, FEA to examine the impact of vehicular in-service loading conditions on the structural behaviour of a hub steering knuckle configuration. The research focused on factors such as the material's density and its ability to withstand stress without permanent deformation. It is logical that the steering knuckle would significantly benefit from optimization in terms of either volume or weight. Similarly, the objective of conducting a static analysis on the steering knuckle is to ascertain the highest levels of stress and deformation that may arise in different scenarios, such as the application of braking force and the transfer of load during acceleration and braking.

2 Materials and Method

The knuckle was designed using SolidWorks 2018. The hub steering knuckle seen in subgraph (a) of Figure 1 was replicated based on the design of the Toyota Camry LE sedan. Materials used for modelling the steering knuckle were aluminium alloy A356.0-T6 and grey cast iron, and their properties are presented in Table 1.

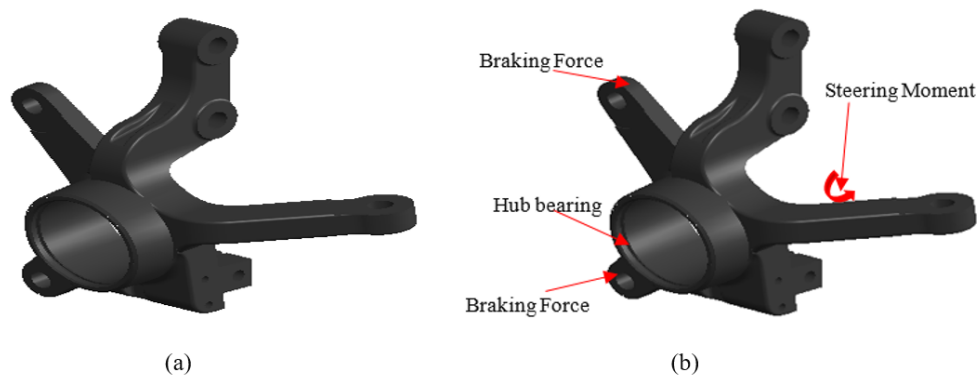


Figure 1. (a) Steering knuckle model; (b) Forces acting on the steering knuckle

Table 1. Properties of materials used for modelling the hub steering knuckle

S/N	Aluminium Alloy A356.0-T6		Grey Cast Iron	
	Material Properties	Values	Material Properties	Values
1.	Density	2670 kg/m^3	Density	7200 kg/m^3
2.	Ultimate tensile strength	234 MPa	Ultimate tensile strength	200-400 MPa
3.	Yield strength	165 MPa	Yield strength	150-250 MPa
4.	Elongation at break	3.5%	Elongation at break	1-3%
5.	Shear modulus	27.2 GPa	Shear modulus	60-80 GPa
6.	Shear strength	143 MPa	Shear strength	300 MPa
7.	Tensile modulus	72.4 GPa	Tensile modulus	170 GPa
8.	Hardness (Brinell)	70 to 105 HB	Hardness (Brinell)	180-220 HB

The knuckle was designed using SolidWorks 2018 and subsequently analysed using the ANSYS R15.0 workstation. This study analysed the design and functionality of the hub-type steering knuckle utilising FEA, a robust engineering tool for simulating the behaviour of intricate structures under diverse loading scenarios. However, it is important

to note that FEA is a numerical method that relies on a number of assumptions and simplifications, and the results should be interpreted with caution. By dividing the structure into small elements and solving the governing equations, FEA provided detailed information about the deformations, stress and strain distribution within the hub steering knuckle at different points along its surface. Multiple loads that are translated in different directions (lateral and multiaxial forces) to the knuckle during service conditions are shown in subgraph (b) of Figure 1.

The part assembly drawing of the steering knuckle, including measurements, is depicted in Figure 2, and the mesh visualization of the steering knuckle is illustrated in Figure 3. There were 116,048 nodes and 76,870 elements in the ANSYS Workbench mechanical meshing, which used a fine relevance center and gradual element transition. A solid mesh was chosen as the mesh type, while a blended curvature-based mesher was utilized.

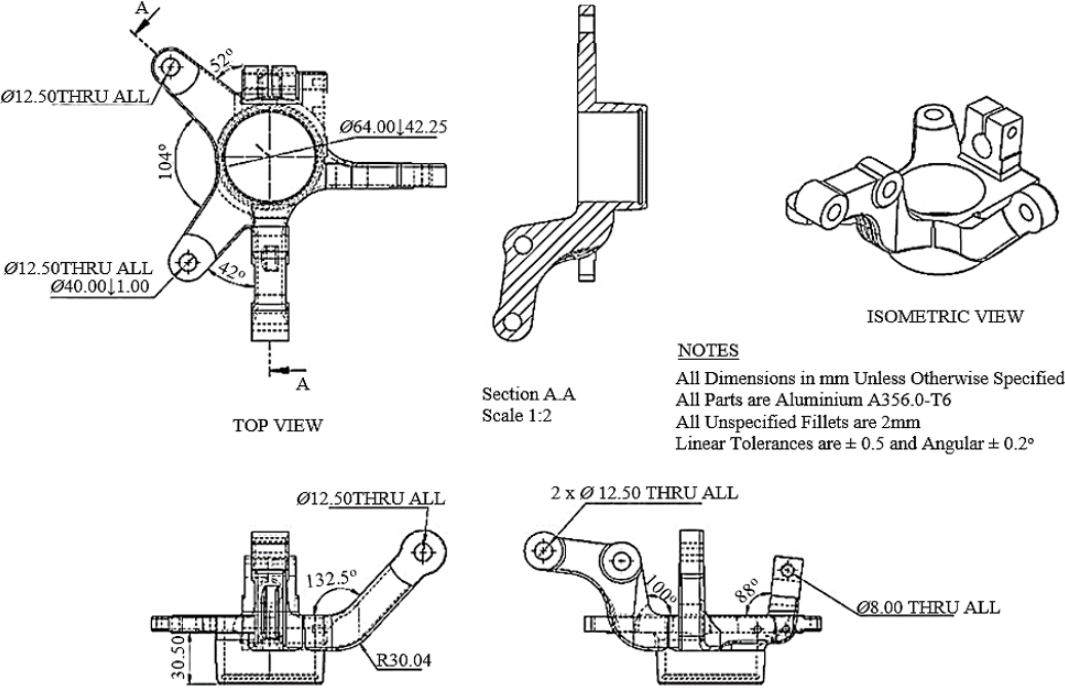


Figure 2. Sketches for steering knuckle with dimensions [24]

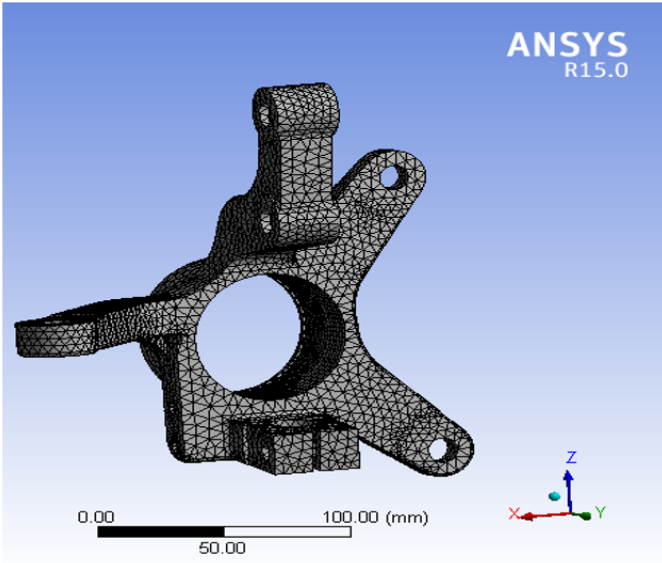


Figure 3. Mesh visualization of the steering knuckle

2.1 Loads/Forces Acting on the Steering Knuckle

The steering knuckle experiences two primary types of loads: tensile and compressive, along with additional multi-translational loads, including lateral and multiaxial forces [24]. The stress resulting from these loads can be calculated using the equations that follow:

$$\text{Tensile load } (P_t) = \text{Tensile stress} * \text{Area} \quad (1)$$

$$\text{Compressive stress } (P_c) = \text{Compressive stress} * \text{Area} \quad (2)$$

Inertia load is an additional type of load exerted on the steering knuckle, resulting from the momentum of moving components. The following expression in Eqs. (3) and (4) provides the basis for the inertia load:

$$\text{Inertia load } (F_a) = \omega^2 R \left[\cos\theta + \frac{R}{L} \cos(2\theta) \right] \quad (3)$$

$$\text{Bending load } (F_b) = \frac{\rho A t L \sin(\theta + \emptyset)}{2} N \quad (4)$$

Stress can be described as the resisting force per unit area that a body exerts against deformation. The necessary information is provided by Eq. (5):

$$\text{Stress}(\sigma) = \frac{P}{A} \quad (5)$$

The inertia bending load induces a tensile stress on one flank of the steering knuckle and a compressive stress on the opposite side, with the sign of this stress alternating with each half revolution [4]. The bending moment at any segment from the smaller end is expressed by Eq. (6):

$$M = \frac{x}{a} \left[1 - \frac{x^2}{L^2} \right] \quad (6)$$

The stress could be computed using the following Eq. (7):

$$\sigma_B = \frac{M}{z} \quad (7)$$

$$M = \frac{I}{2.5} \times t \quad (8)$$

$$I = 419 \times t^4 \quad (9)$$

The steering knuckle is subject to a number of multi-translated loads (lateral and multiaxial forces), which are highlighted as follows:

- i. Forces on Hub Bearing
- ii. Steering Moment
- iii. Braking Force

The analysis seeks to examine the influence of these variables on the model. The analysis seeks to examine the influence of these variables on the model. A static structural analysis was conducted to assess the impact of various forces and moments on the knuckle. The model was created in SolidWorks 2018, and the analysis was conducted via ANSYS 2019 R1.

i. Load on the Hub Bearing

The load on the hub signifies the vehicle's weight, uniformly distributed over the four tires. The load model employed for the investigation was 1606 kg, representing the car's dead weight; hence, the aggregate weight on the knuckle hub was $1606/4 = 401.5$ kg. The cumulative force on the hub was documented as (acting in the Z direction): $401.5 \times 9.81 = 3938.715$ N.

ii. Steering Moment

A minimal steering force of 50 N is often necessary to manoeuvre the steering arm. Consequently, the moment from the force is increased by the parallel distance of 108 mm. The moment was computed as: $50 \times 108 = 5400$ N·mm

iii. The Braking Force

The braking force on the wheel was calculated using Eq. (10).

$$F = \frac{mv^2}{2D} \quad (10)$$

where, F is the braking force, m is the mass of the vehicle =1606 kg, v is the velocity of the vehicle (maximum) = 44.44 (160 Km/h) and D is the braking distance =100 m.

$$F = \frac{401.5 \times 44.44^2}{2 \times 100} = 3964.63 \quad (11)$$

$$\text{Braking moment} = F \times d = 3964.63 \times 70.04 = 277,524.73 \text{ N.mm} \quad (12)$$

Gravity was adjusted to accurately consider inertia. Figure 4 illustrates the model loads of the steering knuckle under static conditions, whereas Table 2 provides the load summary of the steering knuckle model. The detailed explanation of moment, standard earth gravity, forces, loads, and fixed support in the FEA of a hub steering knuckle is essential for analysing its structural behaviour in service conditions.

i. Moment is a measure of the tendency of a force to rotate an object around an axis. In the case of a hub steering knuckle, moments can be applied to simulate the effects of steering and braking forces on the component. These moments are crucial in determining the structural integrity and performance of the knuckle under different operating conditions.

ii. Standard earth gravity, also known as gravitational acceleration, is the acceleration experienced by an object due to the gravitational pull of the Earth. In FEA, standard earth gravity is often used as a loading condition to simulate the weight of the vehicle and its occupants on the hub steering knuckle [25]. This helps in evaluating the strength and stability of the knuckle under static loading conditions.

iii. Forces are external influences that act on a structure and cause it to deform or move [26]. In the context of FEA, forces can be applied to simulate various operating conditions such as cornering, acceleration, and braking. These forces play a crucial role in determining the structural response of the hub steering knuckle and are essential for predicting its performance in real-world scenarios.

iv. Loads refer to the combination of forces, moments, torsion, bending and other external influences acting on a structure. In the FEA of a hub steering knuckle, loads are applied to simulate the dynamic behaviour of the component under different operating conditions. By analysing the distribution of loads on the knuckle, engineers can optimize its design for maximum strength and durability.

v. Fixed support is a boundary condition that restricts the movement of a structure in a specific direction [27]. In the FEA of a hub steering knuckle, fixed supports are used to simulate the mounting points of the knuckle on the vehicle chassis. These supports play a crucial role in determining the structural response of the knuckle under various loading conditions and are essential for ensuring its stability and performance.

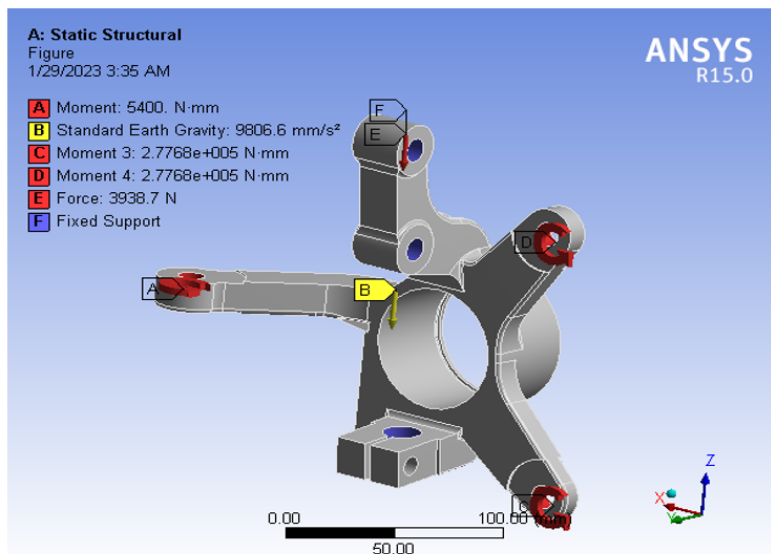


Figure 4. Model loads of the steering knuckle under static condition

Table 2. Load summary of the steering knuckle model

Object Name	Fixed Support	Steering Moment	Braking Moment	Hub Loading
State	Fully Defined	Fully Defined	Fully Defined	Fully Defined
Geometry	3 Faces	1 Face	2 Faces	1 Face
Type	Fixed Support	Moment	Moment	Force
Suppressed	No	No	No	No
Define By		Vector	Vector	Components
Coordinate System				
X Component				
Y Component				
Z Component				-3938.7N (ramped)
Magnitude		5400. N.mm (ramped)	277,524.73 N.mm (ramped)	
Direction		Defined	Defined	

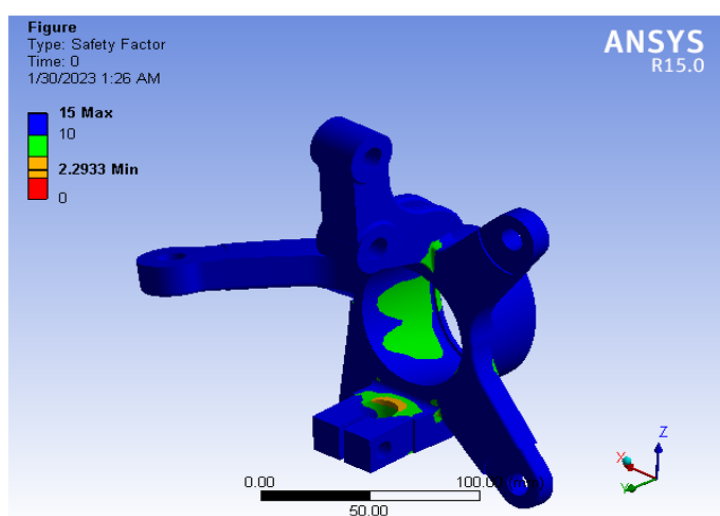


Figure 5. Plot showing FOS profile

Mechanical failures associated with automobiles are frequently ascribed to the deterioration of two interacting components, subpar design or manufacturing flaws, inadequate inspection or maintenance, and other factors [28]. This study analyzed the steering knuckle component utilizing ANSYS Workbench 15.0. The load applied to the component was assessed by reviewing current literature. The average weight of autos was calculated at 1606 kg, according to these figures. The weight is uniformly allocated across all four knuckles, leading to a load of 401.5 kg per tire. The average force exerted on each wheel was 3041.1 N, considering the influence of gravity's acceleration. The knuckle was assumed to be susceptible to several types of loads, including lateral and multiaxial forces like braking forces, moment, torsion, shear forces, lateral forces, and steering forces. Additionally, it experienced loads in the X, Y, and Z axes. The FOS used for the steering knuckle simulation ranged from 2.293 to 15, as seen in Figure 5. A value within this range, which is representative of the simulated component, had significant implications. The FOS in FEA of hub steering knuckles is a crucial parameter that must be carefully considered during the design and analysis process. An FOS greater than 1 indicates that the structure is capable of withstanding the applied loads without failure, while an FOS less than 1 indicates that the structure is at risk of failure [29]. However, a very high FOS in FEA of hub steering knuckles can lead to overdesign and unnecessary weight, which can impact the performance and fuel efficiency of the vehicle. While it is true that a higher FOS may result in a slightly heavier component, the benefits of increased safety and reliability far outweigh the potential drawbacks. Furthermore, advancements in materials and manufacturing techniques have made it possible to design lightweight yet strong hub steering knuckles that meet the required FOS without compromising performance [30]. Based on the colour distribution profile in Figure 5, the steering knuckle model mostly exhibits a royal blue colour. Subsequently, there is a lemon hue with a value of 10 in the centre, accompanied by a slight orange tint (valued at 2.293) in the bottom. The profile indicates that the red hue, denoted by the number zero, has the lowest magnitude. The primary colour on the model is royal

blue, indicating a maximum value of 15. Choosing a factor of safety (FOS) of around 15 for the steering knuckle design can yield a superior quality item compared to employing a FOS of 10. A steering knuckle engineered with a factor of safety (FOS) of 10 will exhibit superior quality compared to one developed with a FOS of 2.293, the minimum value indicated on the colour profile in Figure 5. It is important to note that a steering knuckle with a greater FOS indicates superior quality, but also comes with a higher price.

3 Results and Discussion

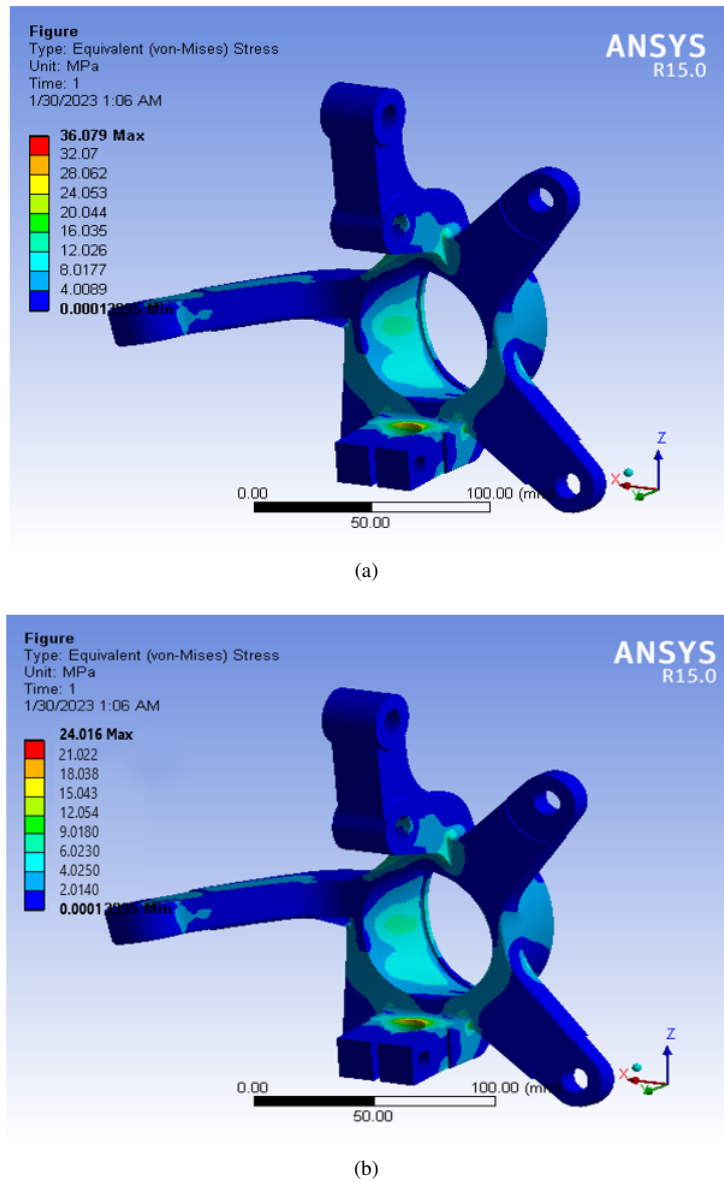
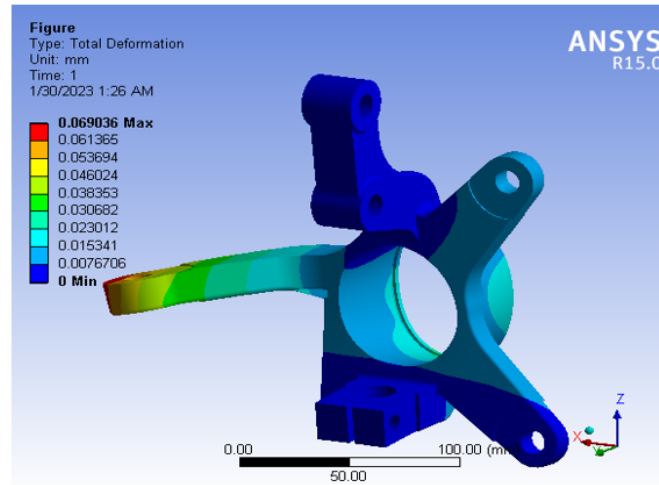


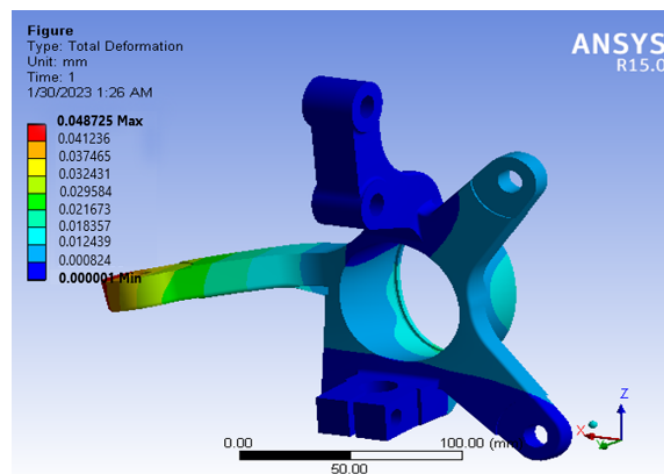
Figure 6. (a) Equivalent VMS profile (A356.0-T6); (b): Equivalent VMS profile (grey cast iron)

The equivalent VMS is a crucial parameter in the operation of a hub steering knuckle, which is a critical component in automotive suspension systems. The VMS is a scalar quantity that represents the equivalent stress in a material, taking into account both the normal and shear stresses acting on a point, and is commonly used to assess the structural integrity of a component [31]. The plot of the simulated equivalent VMS profile of the hub steering knuckle provides valuable insights into the areas of the component that are subjected to the highest levels of stress. In the plot (see Figure 6), VMS is typically represented by a colour scale, with red indicating areas of high stress and blue indicating areas of low stress. The distribution of stress across the component can vary significantly, depending on factors such as the material properties, loading conditions, and geometry of the knuckle. One of the key advantages of using FEA to analyze the stress distribution in the hub steering knuckle is the ability to simulate real-world operating conditions and predict how the component will perform under different loading scenarios. This allows engineers to optimize the

design of the knuckle to ensure that it can withstand the forces and vibrations experienced during normal operation. According to the VMS failure criterion, a given material is deemed to be in a condition of failure when the VMS induced by the applied force above the yield strength of such material. On the other hand, if the VMS value is beneath the material's yield strength, such material is considered to have more strength to withstand additional forces prior to ultimately yielding [32, 33]. This pertains to the concept of material elasticity, which asserts that a material may endure additional loads or stresses provided its elastic limit is not surpassed. It is particularly useful for predicting the onset of yielding and plastic deformation in ductile materials, where the failure is often governed by the overall stress state rather than individual stress components. The VMS considers the overall stress state to predict material failure, while also being more appropriate for ductile materials that exhibit plastic deformation before failure, such as metals.



(a)



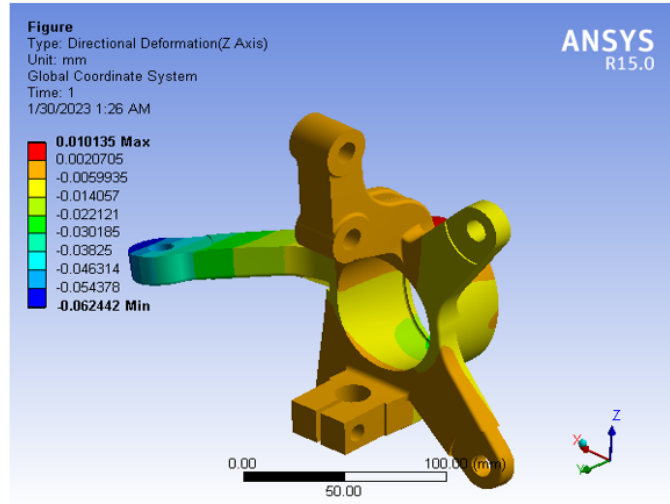
(b)

Figure 7. (a): Plot of total deformation profile (A356.0-T6); (b): Plot of total deformation profile (grey cast iron)

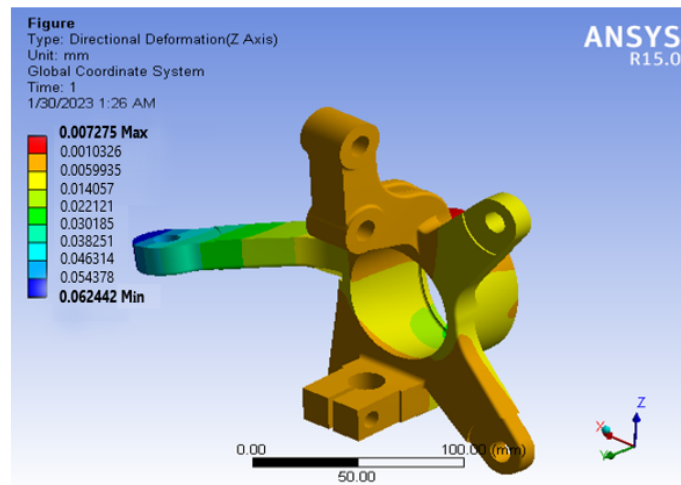
In this study, FEA was used to find the total deformation profile, which gives important information about the steering knuckle's structural integrity and how well it works in different situations. The total deformation profile of the hub steering knuckle is a graphical representation of the displacement of each node in the finite element model [34]. It shows how the structure deforms under applied loads, allowing engineers to identify areas of high stress and potential failure. In the plot of the total deformation profile (see Figure 7), different colours represent different levels of deformation. Areas of high deformation are typically indicated by colours such as red, while areas of low deformation are represented by colours such as blue. By inputting the material properties, boundary conditions, and loading scenarios into the finite element model, the distribution of deformations across the steering knuckle can be examined, and critical areas that may require reinforcement or redesign can be pinpointed. By conducting FEA on the hub steering knuckle, accurate predictions of how the structure will deform and respond to various forces in real-world applications can be made. This information is essential for optimizing the design of the steering knuckle

and ensuring its performance and reliability in actual scenarios.

The directional deformation profile of the hub steering knuckle (see Figure 8) reveals how the structure deforms in response to different loading directions. By analysing the plot of directional deformation, areas of high stress concentration and potential failure points can be identified [35, 36]. This information is crucial for optimizing the design of the steering knuckle and ensuring its reliability and safety in operation. The FEA plot of the directional deformation profile of the hub steering knuckle in Figure 8 reveals that the deformation is not uniform across the structure. The plot highlights areas of localized deformation, indicating regions of high stress concentration. This information indicates the potential weak points in the design, implying that necessary modifications are required to improve the structural integrity of the steering knuckle.



(a)



(b)

Figure 8. (a): Directional deformation (bending along Z-axis) profile (A356.0-T6); (b): Directional deformation (bending along Z-axis) profile (grey cast iron)

The static study depicted in Figure 6 yielded a peak equivalent VMS of 36.079 MPa for the steering knuckle constructed from aluminium alloy A356.0-T, which possesses a yield strength of 165 MPa. A peak VMS of 24.016 MPa was recorded for the steering knuckle designed from grey cast iron, which had a yield strength of 200 MPa. The peak simulated VMS for both materials is obviously below their yield strength (refer to Figure 9), indicating that the component is unlikely to break under the applied load conditions. The A356.0-T steering knuckle experienced total deformation in two ways: it deformed along the Z-axis by 0.010135 mm (shown in subgraph (a) of Figure 7) and also deformed in one direction by 0.069036 mm (shown in subgraph (a) of Figure 8). A total deformation of 0.048725 mm was measured for the grey cast iron steering knuckle, which can be seen in subgraph (b) of Figure 7. The same part also showed directional deformation (bending along the Z-axis) of 0.007275 mm, which can be seen in subgraph (b) of Figure 8. This suggests that the aforementioned deformation is unlikely to have any detrimental impact on the

component, since both materials retain the capacity to endure further stresses or loads prior to yielding or failure. Comparing the performance of both materials under the applied load conditions, it is observed that the VMS, total and directional deformation values (see Figure 6, Figure 7, and Figure 8) obtained for the hub steering knuckle that was modelled with grey cast iron are lower than those modelled with A356.0-T. Making reference to the theory of VMS failure criterion, grey cast iron, which has a higher yield strength property, may last longer and perform better than a steering knuckle designed with A356.0-T.

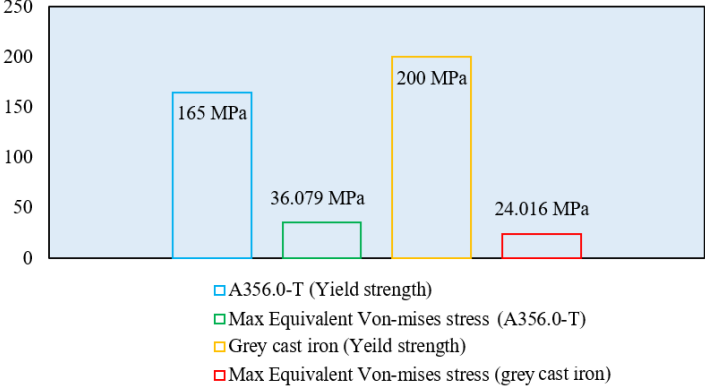
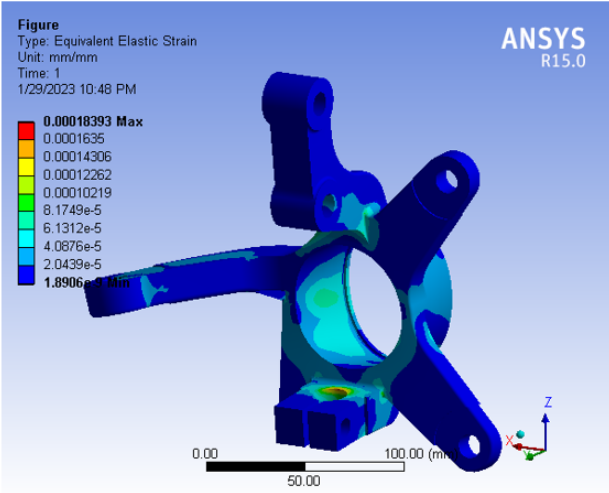
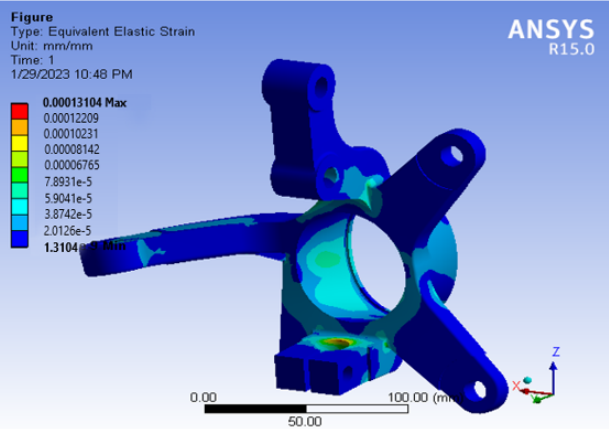


Figure 9. Plot of maximum equivalent VMS and yield strength for A356.0-T and grey cast iron

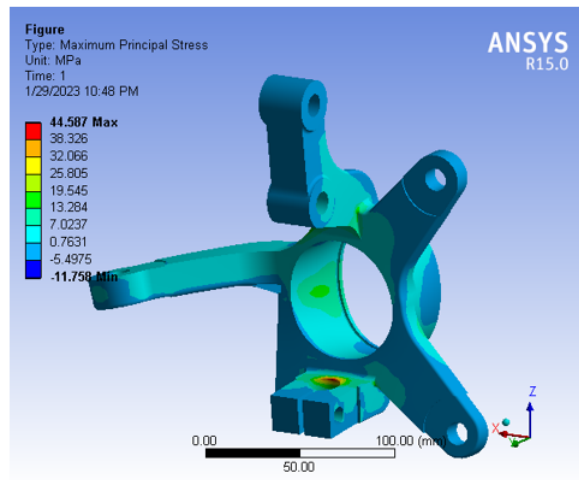


(a)

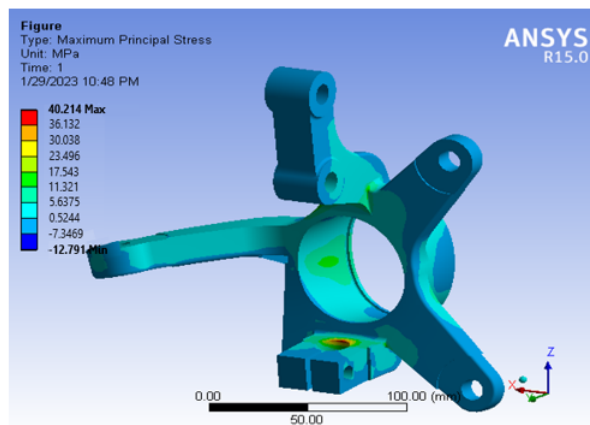


(b)

Figure 10. (a): Equivalent elastic strain profile (A356.0-T); (b): Equivalent elastic strain profile (grey cast iron)



(a)



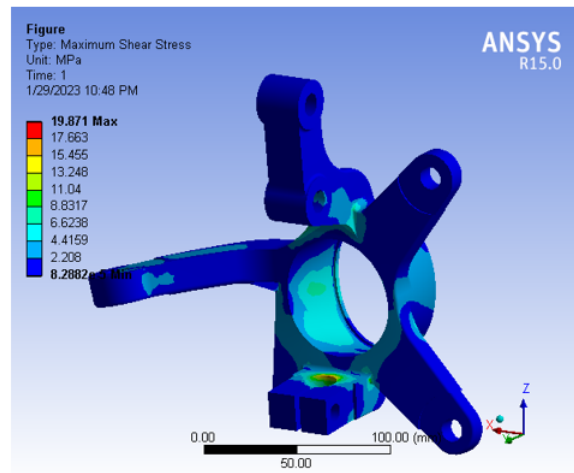
(b)

Figure 11. (a): Maximum principal stress profile (A356.0-T); (b): Maximum principal stress profile (grey cast iron)

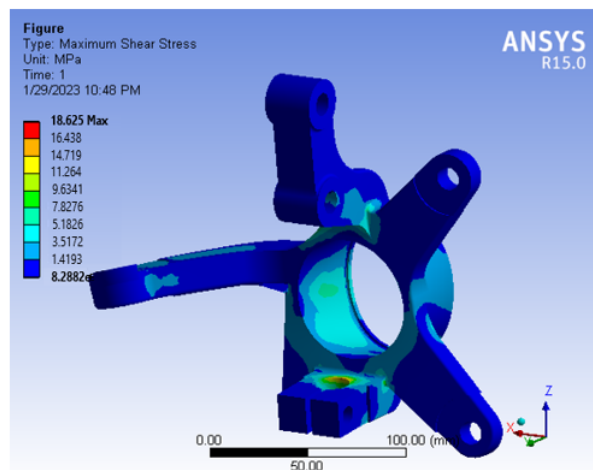
Vibration, steering displacement, temperature, corrosion, and various external and internal forces exert stress on the steering knuckle, ultimately resulting in a strain deformation of the material. This is defined by geometric distortion indicating the relative movement of particles within the component. The aforementioned deformation can be seen as elongations resulting from the dislocation of atoms inside the metal lattice and is contingent upon the trajectory of forces acting on it [37]. Under severe circumstances involving uneven road surfaces with potholes and speed bumps, the steering knuckle may experience cyclic stress, resulting in variable elastic strain. This is a measure of deformation in a material, and understanding how it is distributed across a component can help engineers identify potential areas of weakness or failure on the knuckle system that may result in bending deformation and possibly lead to fatigue [38]. The simulated maximum equivalent elastic strain profiles for A356.0-T and grey cast iron are shown in Figure 10. The equivalent elastic strain profile provides valuable insights into the distribution of strain within the hub steering knuckle. From the profiles, a maximum equivalent strain of 0.00018393 mm/mm was obtained for A356.0-T as shown in subgraph (a) of Figure 10, while the maximum simulated principal stress of 0.00013104 mm/mm was obtained for grey cast iron as shown in subgraph (b) of Figure 10. Comparing the maximum equivalent strains obtained for both materials operating under the same loading conditions, grey cast iron exhibited lower principal stresses. This implies that for a hub steering knuckle designed with both materials and operating under the same loading condition, A356.0-T will elongate faster and may also fail faster than the same component designed with grey cast iron. This is due to the difference in the material properties. The plot shows that the highest strains are concentrated near the points where the knuckle is connected to other components, such as the wheel hub and the steering linkage.

The plot of the maximum principal stress profile of the hub steering knuckle (see Figure 11) shows the distribution of stress throughout the component. The stress is represented by a colour scale, with red indicating high stress levels and blue indicating low stress levels. In the field of mechanics and materials science, the concept of maximum principal stress is commonly used to analyse the stress distribution in a material under loading conditions. While both

measures provide valuable information about the state of stress in a material, they are fundamentally different in their approach and interpretation. Maximum principal stress is a scalar quantity that represents the maximum value of the normal stress acting on a specific plane within a material [39, 40]. In other words, they are stresses that correspond to normal stresses on the major planes exhibiting minimal shear stress. These planes are orthogonal to the primary directions along which the principal stresses act [41]. It is derived from the three principal stresses that characterize the stress state at a given point. While maximum principal stress focuses on the critical normal stress acting on a specific plane, in practical terms, it is also more suitable for brittle materials that fail in a brittle manner [42]. The maximum principal stress is important because it indicates the likelihood of failure in a material due to tensile or compressive loading. Engineers often use this measure to design structures and components that can withstand the highest stress levels without experiencing failure. The maximum principal stresses $\sigma_1 \geq \sigma_2 \geq \sigma_3$ obtained from the simulation of a hub steering knuckle modelled with A356.0-T and grey cast iron are shown in Figure 11. From the profile, a maximum simulated principal stress of 44.587 MPa was obtained for A356.0-T as shown in subgraph (a) of Figure 11, while the maximum simulated principal stress of 40.214 MPa was obtained for grey cast iron as shown in subgraph (b) of Figure 11. Comparing the maximum principal stresses obtained for both materials operating under the same loading conditions, grey cast iron obviously exhibited lower principal stresses, indicating that a hub steering knuckle designed with A356.0-T under the same loading condition will fail earlier than grey cast iron. This is as a result of the mechanical properties of grey cast iron which outweigh the properties of A356.0-T.



(a)



(b)

Figure 12. (a): Maximum shear stress profile (A356.0-T); (b): Maximum shear stress profile (grey cast iron)

Although initially negligible, shear stress is generated on the steering knuckle during each cornering cycle performed by the steering components. However, it gradually becomes substantial after the component has undergone thousands to millions of vibrational and frequency cycles. This due to persistent exposure to multi-translational loads acting on the vehicle suspension [43]. Shear stress is a fundamental concept in the field of mechanics, particularly in

the study of fluid dynamics and solid mechanics. It is defined as the force per unit area that acts parallel to a surface, causing deformation or displacement within the material [44, 45]. Shear stress plays a crucial role in determining the behaviour of materials under various loading conditions, and understanding its principles is essential for engineers to optimize the design of the knuckle and ensure that it can withstand the expected loads without failure. The principles of shear stress are based on the fundamental laws of physics, specifically Newton's third law of motion, which states that for every action, there is an equal and opposite reaction [46]. In the context of shear stress, this means that when a force is applied parallel to a surface of the steering knuckle, it creates a shearing force that causes the material to deform or move. The magnitude of shear stress is directly proportional to the applied force and inversely proportional to the cross-sectional area over which it is applied. The simulated maximum shear stress profiles for A356.0-T and grey cast iron materials are presented in Figure 12.

From the simulated profile in Figure 12, a maximum shear stress of 19.871 MPa was obtained for the steering knuckle designed with A356.0-T material, while 18.625 MPa was obtained for the steering knuckle designed with grey cast iron. These numbers show the loads or forces per unit area that tend to bend the steering knuckle by letting it slip along the planes that are parallel to the stresses that are being put on it. Comparatively, the maximum shear stress obtained for a steering knuckle designed with A356.0-T material will induce failure or expose the component to failure earlier than grey cast iron under the same operating load conditions. This is as a result of the mechanical properties of grey cast iron, which outweigh the properties of A356.0-T. Hence, the shear stress profile of the hub steering knuckle is influenced by several factors, including the geometry of the knuckle, the material properties, and the loading conditions.

4 Manufacturing Process of Hub Steering Knuckle

The manufacturing process of hub steering knuckles involves the following intricate steps, including cutting, forging, joining, and machining techniques. This process is crucial in the production of high-quality steering knuckles, which are essential components in the automotive industry.

i. The first step in the manufacturing process of an automobile steering knuckle is the selection of the raw materials. Typically, steering knuckles are made from high-strength steel or aluminium alloys, chosen for their durability and ability to withstand the stresses and strains of daily use. The raw materials are carefully inspected for any defects or impurities before being processed further.

ii. The next step in the manufacturing process of hub steering knuckles is cutting. This involves the use of specialized cutting tools to shape the raw material into the desired form. The cutting process is crucial in ensuring that the steering knuckle is of the correct size and shape, as any inaccuracies at this stage can lead to defects in the final product. Precision cutting techniques are used to ensure that the steering knuckle meets the required specifications. This step is crucial in ensuring that the steering knuckle has the correct dimensions and geometry to fit seamlessly into the vehicle's steering system. Precision is key in this step, as even minor deviations from the required specifications can lead to issues with the steering performance of the vehicle.

iii. After the cutting stage, the next step in the manufacturing process is forging. Forging involves the application of heat and pressure to improve the mechanical properties and enhance the strength and durability of the steering knuckle by shaping it into the desired form. The forging process also helps to eliminate any defects in the material, ensuring that the steering knuckle is of high quality and durability to withstand the forces and loads it will experience during normal operation.

iv. Once the forging process is complete, the next step in the manufacturing process is joining. Joining involves the assembly of different components of the steering knuckle using welding or other joining techniques. This stage is crucial in ensuring that the steering knuckle is structurally sound and able to withstand the rigors of use in automotive applications. Welding is used to join the various components of the knuckle, such as the hub, steering arm, and spindle. The most common welding techniques used in the manufacturing of hub steering knuckles are MIG (Metal Inert Gas) welding and TIG (Tungsten Inert Gas) welding. MIG welding is preferred for its speed and efficiency, while TIG welding is used for its precision and control, with no weak points or defects.

v. The next step in the manufacturing process of hub steering knuckles is machining. Machining involves the use of precision tools and techniques to shape and finish the steering knuckle to the required specifications. Machining is a key aspect of the finishing process, as it involves shaping and refining the assembled steering knuckle to meet the required dimensions and tolerances. This process typically involves cutting, drilling, milling, and grinding operations to achieve the desired shape and surface finish of the steering knuckle. Precision machining is essential to ensure that the steering knuckle fits accurately and functions properly within the vehicle's suspension system. This stage is crucial in ensuring that the component is of the correct size and shape, with smooth surfaces and precise dimensions.

vi. In addition to machining, coatings are also applied to the steering knuckle to enhance its durability, corrosion resistance, and aesthetics. Coatings such as powder coating, electroplating, and painting are commonly used to protect the steering knuckle from environmental factors and improve its appearance. These coatings not only provide a protective barrier against rust and wear but also contribute to the overall aesthetics of the steering knuckle.

Each stage of the process is crucial in ensuring that the steering knuckle is of high quality and durability, meeting the required specifications for use in automotive applications. Precision and quality control are essential throughout the manufacturing process to ensure that the steering knuckle meets the highest standards of performance and reliability.

5 Causes of Hub Steering Knuckle Failure

Steering knuckle failure is a common issue that can occur in vehicles, leading to potential safety hazards and costly repairs. There are several factors that can contribute to the failure of steering knuckles, including wear and tear, improper maintenance, and manufacturing defects [9]. Like any mechanical part, the hub steering knuckle is susceptible to failure due to a variety of factors detailed as follows:

i. One of the primary causes of failure in hub steering knuckles is wear and tear due to normal use and age. Over time, the constant stress and strain placed on the knuckle can lead to fatigue and eventual failure. This can be exacerbated by poor maintenance practices, such as failing to lubricate the knuckle regularly or ignoring signs of wear and damage. In addition, exposure to harsh environmental conditions, such as extreme temperatures and road salt, can accelerate the deterioration of the knuckle and increase the likelihood of failure.

ii. Another common cause of failure in hub steering knuckles is impact damage, such as hitting a pothole or curb at high speeds. This can cause the knuckle to bend or crack, compromising its structural integrity and leading to steering issues and potential safety hazards. Improper installation or alignment of the knuckle can also contribute to failure, as misalignment can put additional stress on the component and cause premature wear and damage.

iii. Improper maintenance is another common cause of steering knuckle failure. Failure to properly lubricate the steering knuckle or neglecting to replace worn out components can lead to increased stress on the knuckle, ultimately causing it to fail. It is important for vehicle owners to follow the manufacturer's recommended maintenance schedule and to address any issues promptly to prevent steering knuckle failure.

iv. Manufacturing defects can also contribute to steering knuckle failure. In some cases, the steering knuckle may have been improperly manufactured or installed, leading to premature failure. This can be difficult to detect, as the issue may not present itself until the vehicle is in use. However, regular inspections and maintenance can help to identify any potential defects early on, allowing for repairs or replacements to be made before a failure occurs.

The causes of failure in hub steering knuckles are varied and complex, encompassing factors such as wear and tear, impact damage, poor maintenance practices, improper installation, and manufacturing defects. By understanding these causes and taking proactive measures to address them, vehicle owners and mechanics can prevent costly repairs and ensure the safe and efficient operation of the steering system. Regular inspection, maintenance, and replacement of worn or damaged components are essential to prolonging the lifespan of hub steering knuckles and maintaining the overall performance and safety of the vehicle.

6 Failure Prevention Techniques in Hub Steering Knuckle

Failure prevention techniques in hub steering knuckles are crucial for ensuring the safety and reliability of vehicles [47, 48]. There are various methods that can be employed to prevent such failures, ranging from regular maintenance to using high-quality materials. These are highlighted as follows:

i. One of the most common causes of failure in hub steering knuckles is fatigue failure. This occurs when the knuckle is subjected to repeated loading and unloading, causing it to weaken and eventually break. To prevent fatigue failure, manufacturers use high-quality materials such as forged steel or aluminium, which have high strength and fatigue resistance. Additionally, the design of the knuckle is optimized to distribute the load evenly and minimize stress concentrations.

ii. Another method for preventing failures in hub steering knuckles is using high-quality materials. Knuckles that are made from high-quality materials, such as forged steel or aluminium, are less likely to fail than those made from lower-quality materials. By investing in high-quality materials, vehicle owners can help to prevent failures in hub steering knuckles and ensure the safety and performance of their vehicles.

iii. Another important failure prevention technique is regular inspection and maintenance. Inspecting the hub steering knuckles for signs of wear, corrosion, or damage can help identify potential issues before they escalate into major problems. Regular maintenance, such as lubricating the joints and replacing worn-out components, can also extend the lifespan of the knuckle and prevent premature failure.

iv. In addition to material selection and maintenance, proper installation and assembly are essential for preventing failure in hub steering knuckles. Incorrect installation can lead to misalignment, uneven loading, and increased stress on the knuckle, which can compromise its structural integrity. Following manufacturer guidelines and using proper tools and techniques during installation can help ensure that the knuckle is properly aligned and securely attached to the vehicle.

Overall, failure prevention techniques in hub steering knuckles are essential for maintaining the safety and performance of vehicles. By using high-quality materials, conducting regular inspections and maintenance, and ensuring proper installation, manufacturers can minimize the risk of failure and prolong the lifespan of the knuckle.

Investing in failure prevention techniques not only improves the reliability of vehicles but also reduces the risk of accidents and costly repairs.

7 Conclusions

This study centred on FEA of vehicular in-service loading effects in relation to static-structural behaviour of a hub steering knuckle configuration, considering two commonly used materials for manufacturing vehicle hub steering knuckles, including grey cast iron and aluminium A356.0-T6. Both materials have their own unique properties and characteristics that make them suitable for hub steering knuckles. It was observed that grey cast iron is a popular material choice for vehicle components due to its high strength, wear and resistance, and damping capacity. Moreover, it is also relatively inexpensive and easy to cast, making it a cost-effective option for mass production. On the other hand, aluminium A356.0-T6 is known for its lightweight properties, high strength-to-weight ratio, and excellent corrosion resistance. It is commonly used on hub steering knuckles when weight reduction is a priority. This is evident in the FEA results in this study, where the maximum equivalent VMS, maximum equivalent elastic strain, maximum principal stress, and maximum shear stress of 36.079 MPa, 0.00018393 mm/mm, 44.587 MPa, and 19.871 MPa obtained for A356.0-T were higher than these same parameters of 24.016 MPa, 0.00013104 mm/mm, 41.214 MPa, and 18.625 MPa obtained for grey cast iron. The results obviously support the claim that grey cast iron is a superior material for steering knuckle applications, despite its high density. This study further revealed that one key difference between grey cast iron and aluminium A356.0-T6 is their weight. Grey cast iron is significantly heavier than aluminium A356.0-T6, which can impact the overall fuel efficiency and performance of the vehicle. In applications where weight reduction is a priority, aluminium A356.0-T6 may be the preferred choice due to its lightweight properties.

Furthermore, grey cast iron has a higher compressive strength and wear resistance compared to aluminium A356.0-T6. This makes it a suitable choice for hub steering knuckles where high strength and durability are required, such as in heavy-duty vehicles. On the other hand, aluminium A356.0-T6 has a higher tensile strength and fatigue resistance, making it a better choice for applications where weight reduction and corrosion resistance are important. Ultimately, the decision should be based on a thorough analysis of the specific requirements and performance criteria of the application. However, it is important to note that the choice between these two materials, ultimately the steering knuckle, depends on specific requirements such as weight savings, cost considerations, and performance requirements. Based on the insights derived from this study, the following recommendations may aid manufacturers in enhancing the standard of hub steering knuckles for optimal vehicle performance:

i. It is essential to consider the material properties of the hub steering knuckle when conducting FEA studies. The choice of material can significantly impact the structural behaviour and performance of the component. Therefore, it is crucial to select a material that can withstand the expected loading conditions while maintaining the required strength and durability. Additionally, the material properties should be accurately defined in the FEA model to ensure accurate predictions of the component's behaviour.

ii. The boundary conditions and loading conditions applied in the FEA model should closely emulate the actual in-service conditions experienced by the hub steering knuckle. This includes considering factors such as road conditions, vehicle speed, and steering manoeuvres. By accurately simulating these conditions, the FEA model can provide more realistic predictions of the component's behaviour and performance.

iii. It is important to conduct sensitivity analyses to identify critical areas of the hub steering knuckle that may be prone to failure under certain loading conditions. By identifying these areas, designers can implement targeted design modifications to improve the overall strength and durability of the component. Additionally, fatigue analysis should be performed to assess the component's fatigue life under repeated loading conditions, which is crucial for ensuring the long-term reliability of the hub steering knuckle.

These studies on the FEA of hub steering knuckle configurations have provided valuable insights into the static-structural behaviour in its in-service loading conditions. By following the recommendations outlined, engineers can improve the design and performance of hub steering knuckles, ultimately enhancing the safety and reliability of vehicles. Continuous research is essential in this area to further advance the present body of knowledge on the structural behaviour of the hub steering knuckle and improve overall vehicle performance.

Data Availability

The data used to support the research findings are available from the corresponding author upon request.

Conflicts of Interest

The authors declare no conflict of interest.

References

- [1] L. R. Kumar, S. Sivalingam, K. Prashanth, and K. Rajkumar, "Design, analysis and optimization of steering knuckle for all terrain vehicles," *AIP Conf. Proc.*, vol. 2207, p. 020003, 2020. <http://doi.org/10.1063/5.0000044>
- [2] K. K. Reza, "Failure strength of automotive steering knuckle made of metal matrix composite," *Appl. Mech.*, vol. 4, no. 1, pp. 210–229, 2023. <http://doi.org/10.3390/applmech4010012>
- [3] V. Dhinakaran, A. R. Kumar, R. Ramgopal, S. Kannan, B. Stalin, and T. Jagadeesha, "Topology optimization of steering knuckle," in *Advances in Industrial Automation and Smart Manufacturing*, 2021, pp. 197–206. http://doi.org/10.1007/978-981-15-4739-3_17
- [4] B. Babu, M. Prabhu, P. Dharmaraj, and R. Sampath, "Stress analysis on steering knuckle of the automobile steering system," *Int. J. Res. Eng. Tech.*, vol. 3, no. 3, pp. 363–366, 2014. <http://doi.org/10.15623/ijret.2014.0303067>
- [5] E. A. Azrulhisham, Y. M. Asri, A. W. Dzuraidah, N. M. Nik Abdullah, and C. H. Che Hassan, "Evaluation of fatigue life reliability of steering knuckle using pearson parametric distribution model," *Int. J. Qual. Stat. Relia.*, vol. 10, pp. 1–8, 2010. <http://doi.org/10.1155/2010/816407>
- [6] T. V. Do, T. M. Pham, and H. Hao, "Dynamic responses and failure modes of bridge columns under vehicle collision," *Eng. Struct.*, vol. 156, pp. 243–259, 2018. <http://doi.org/10.1016/j.engstruct.2017.11.053>
- [7] D. Saddington, "The global chassis sector report: An analysis of the braking, steering and suspension markets," SAE Technical Paper, MR-AB-017, Tech. Rep., 2015.
- [8] M. Zoroufi and A. Fatemi, "Experimental durability assessment and life prediction of vehicle suspension components: A case study of steering knuckles," *Proc. Inst. Mech. Engrs., Part D: J. Autom. Eng.*, vol. 220, no. 11, pp. 1565–1579, 2006. <http://doi.org/10.1243/09544070JAUTO310>
- [9] S. Y. Raj, H. P. Dayalan, and M. Shrivardhan, "Investigation of knuckle joint and its importance — A literature case study," in *2018 7th International Conference on Industrial Technology and Management (ICITM)*, Oxford, UK, 2018, pp. 62–70. <http://doi.org/10.1109/ICITM.2018.8333921>
- [10] K. K. Reza, K. Souiri, B. A. Gharehsheikh, J. R. Safavi, and M. Ahmad, "Fatigue life analysis of automotive cast iron knuckle under constant and variable amplitude loading conditions," *Appl. Mech.*, vol. 3, no. 2, pp. 517–532, 2022. <http://doi.org/10.3390/applmech3020030>
- [11] S. Ranganathan, S. Gopal, S. Eswaran, and S. Muthusamy, "Design and analysis of steering knuckle for FSAE vehicle," *SAE Int. J. Adv. Curr. Prac. Mobil.*, vol. 3, no. 2, pp. 856–863, 2021. <https://doi.org/10.4271/2020-28-0506>
- [12] A. Hasan, C. H. Lu, and W. Liu, "Lightweight design and analysis of steering knuckle of formula student car using topology optimization method," *World Electr. Veh. J.*, vol. 14, no. 9, p. 233, 2023. <https://doi.org/10.3390/wevj14090233>
- [13] M. Zoroufi and A. Fatemi, "Fatigue life comparisons of competing manufacturing processes: A study of steering knuckle," SAE Technical Paper, 2004-01-0628, Tech. Rep., 2004. <https://doi.org/10.4271/2004-01-0628>
- [14] C. Santana, L. Reyes-Osorio, J. Orona-Hinojos, L. Huerta, A. Rios, and P. Zambrano-Robledo, "Numerical study of reinforced aluminum composites for steering knuckles in last-mile electric vehicles," *World Electr. Veh. J.*, vol. 15, no. 3, p. 109, 2024. <https://doi.org/10.3390/wevj15030109>
- [15] F. Li, J. Sun, J. Bao, J. Yang, H. Li, C. Zhong, Y. Gao, Q. He, K. Xie, and W. Li, "Failure analysis of truck steering knuckle," *Eng. Failure Anal.*, vol. 140, p. 106537, 2022. <https://doi.org/10.1016/j.engfailanal.2022.106537>
- [16] P. Dumbre, A. K. Mishra, V. S. Aher, and S. S. Kulkarni, "Structural analysis of steering knuckle for weight reduction," *Int. J. Emerg. Tech. Adv. Eng.*, vol. 4, no. 6, pp. 552–557, 2014.
- [17] W. M. Muhamad, E. Sujatmika, H. Hamid, and F. Tarlochan, "Design improvement of steering knuckle component using shape optimization," *Int. J. Adv. Comp. Sci.*, vol. 2, no. 2, pp. 65–69, 2012.
- [18] M. P. Sharma, D. S. Mevewala, H. Joshi, and D. A. Patel, "Static analysis of steering knuckle and its shape optimization," *J. Mech. Civil Engr.*, vol. 16, pp. 34–38, 2014.
- [19] K. R. Kashyzadeh and G. H. Farrahi, "Improvement of HCF life of automotive safety components considering a novel design of wheel alignment based on a hybrid multibody dynamic, finite element, and data mining techniques," *Eng. Failure Anal.*, vol. 143, p. 106932, 2023. <https://doi.org/10.1016/j.engfailanal.2022.106932>
- [20] S. Liu, G. Zhang, and A. Wang, "Progressive failure mechanism of structuralized cemented slopes," *Engr. Failure Anal.*, vol. 143, p. 106939, 2023. <https://doi.org/10.1016/j.engfailanal.2022.106939>
- [21] S. Yadav, R. K. Mishra, V. Ansari, and S. B. Lal, "Design and analysis of steering knuckle component," *Int. J. Res. Tech.*, vol. 5, no. 4, pp. 457–463, 2016.
- [22] S. V. Dusane, M. K. Dipke, and M. A. Kumbhalkar, "Analysis of steering knuckle of all terrain vehicles (ATV) using finite element analysis," *IOP Conf. Ser.: Mat. Sci. Eng.*, vol. 149, p. 012133, 2016. <https://doi.org/10.1088/1757-899X/149/1/012133>
- [23] K. R. Kashyzadeh, "Failure strength of automotive steering knuckle made of metal matrix composite," *Appl.*

- Mech.*, vol. 4, no. 1, pp. 210–229, 2023. <https://doi.org/10.3390/applmech4010012>
- [24] A. E. Ikpe, M. O. Basse, and E. M. Etuk, “Multiaxial non-proportional random analysis of a typical hub steering knuckle with respect to in-service loading effects on its geometric model,” in *4th International Congress on Natural and Applied Sciences*, Rio de Janeiro, Brazil, 2023, pp. 184–197.
- [25] J. Kurebwa and T. Mushiri, “Design and simulation of an integrated steering system for all-purpose sport utility vehicles (SUVs)–Case for Toyota,” *Proc. Manuf.*, vol. 35, pp. 56–74, 2019. <https://doi.org/10.1016/j.promfg.2019.07.002>
- [26] A. M. Obenaus, M. Y. Mollica, and N. J. Sniadecki, “(De)form and function: Measuring cellular forces with deformable materials and deformable structures,” *Adv. Healthcare Mat.*, vol. 9, no. 8, p. 1901454, 2020. <https://doi.org/10.1002/adhm.201901454>
- [27] J. Bracamonte, J. S. Wilson, and J. S. Soares, “Modeling patient-specific periaortic interactions with static and dynamic structures using a moving heterogeneous elastic foundation boundary condition,” in *Functional Imaging and Modelling of the Heart*, 2021, pp. 315–327. https://doi.org/10.1007/978-3-030-78710-3_31
- [28] A. E. Ikpe, I. B. Owunna, P. O. Egunilo, and E. E. Ikpe, “Static analysis on a vehicle tie rod to determine the resulting buckling displacement,” *Int. J. Ind. Manf. Syst. Engr.*, vol. 1, no. 1, pp. 16–24, 2016. <https://doi.org/10.11648/j.ijimse.20160101.13>
- [29] C. V. Amaechi, C. Chesterton, H. O. Butler, F. Wang, and J. Ye, “An overview on bonded marine hoses for sustainable fluid transfer and (un)loading operations via floating offshore structures (FOS),” *J. Marine Sci. Eng.*, vol. 9, no. 11, p. 1236, 2021. <https://doi.org/10.3390/jmse9111236>
- [30] A. E. Ikpe and I. B. Owunna, “Design of remotely controlled hydraulic bottle jack for automobile applications,” *Int. J. Eng. Res. Dev.*, vol. 11, no. 1, pp. 124–134, 2019. <http://doi.org/10.29137/umagd.440893>
- [31] M. Abambres and M. R. Arruda, “Finite element analysis of steel structures–A review of useful guidelines,” *Int. J. Strut. Integ.*, vol. 7, no. 4, pp. 490–515, 2016. <https://doi.org/10.1108/IJSI-07-2015-0020>
- [32] A. E. Ikpe, I. B. Owunna, and P. O. Egunilo, “Determining the accuracy of finite element analysis when compared to experimental approach for measuring stress and strain on a connecting rod subjected to variable loads,” *J. Robt. Comp. Vis. Graph.*, vol. 1, no. 1, pp. 12–20, 2016.
- [33] A. E. Ikpe and I. Owunna, “Design of vehicle compression springs for optimum performance in their service condition,” *Int. J. Eng. Res. Afr.*, vol. 33, pp. 22–34, 2017. <https://doi.org/10.4028/www.scientific.net/JERA.33.22>
- [34] H. Gupta and N. K. Singh, “Design and analysis of steering knuckle of hybrid metal matrix composite for the FSAE vehicle,” *Mat. Today: Proc.*, vol. 46, pp. 10 551–10 557, 2021. <https://doi.org/10.1016/J.MATPR.2021.01.104>
- [35] B. Cheng, S. Shrestha, and K. Chou, “Stress and deformation evaluations of scanning strategy effect in selective laser melting,” *Additive Manuf.*, vol. 12, pp. 240–251, 2016. <https://doi.org/10.1016/j.addma.2016.05.007>
- [36] N. Gates and A. Fatemi, “Notch deformation and stress gradient effects in multiaxial fatigue,” *Theory Appl. Frac. Mech.*, vol. 84, pp. 3–25, 2016. <https://doi.org/10.1016/j.tafmec.2016.02.005>
- [37] E. M. Etuk, A. E. Ikpe, and U. A. Azum, “Modelling and analysis of 2-stage planetary gear train for modular horizontal wind turbine application,” *J. Appl. Res. Ind. Eng.*, vol. 6, no. 4, pp. 268–282, 2019. <https://doi.org/10.22105/jarie.2020.213154.1114>
- [38] P. Kindt, D. Berckmans, F. De Coninck, P. Sas, and W. Desmet, “Experimental analysis of the structure-borne tyre/road noise due to road discontinuities,” *Mech. Syst. Signal Proc.*, vol. 23, no. 8, pp. 2557–2574, 2009. <https://doi.org/10.1016/j.ymsp.2009.04.005>
- [39] W. F. Chen and A. F. Saleeb, *Constitutive Equations for Engineering Materials: Elasticity and Modelling*. New York: Elsevier Science, 2013.
- [40] R. R. Craig and E. M. Taleff, *Mechanics of Materials*. John Wiley & Sons, 2020.
- [41] W. D. Means, *Stress and Strain: Basic Concepts of Continuum Mechanics for Geologists*. New York: Springer-Verlag, 2012.
- [42] I. R. Kivi, M. Ameri, and H. Molladavoodi, “Shale brittleness evaluation based on energy balance analysis of stress-strain curves,” *J. Pet. Sci. Engr.*, vol. 167, pp. 1–19, 2018. <https://doi.org/10.1016/J.PETROL.2018.03.061>
- [43] D. Lehmus, M. Busse, A. Herrmann, and K. Kayvantash, *Structural Materials and Processes in Transportation*. Weinheim, Germany: Wiley-VCH Verlag GmbH & Co, KGaA, 2013.
- [44] D. Katritsis, L. Kaiktsis, A. Chaniotis, J. Pantos, E. P. Efstathopoulos, and V. Marmarelis, “Wall shear stress: Theoretical considerations and methods of measurement,” *Prog. Cardiovasc. Dis.*, vol. 49, no. 5, pp. 307–329, 2007. <https://doi.org/10.1016/j.pcad.2006.11.001>
- [45] N. J. Balmforth, I. A. Frigaard, and G. Ovarlez, “Yielding to stress: Recent developments in viscoplastic fluid mechanics,” *Annu. Rev. Fluid Mech.*, vol. 46, pp. 121–146, 2014. <https://doi.org/10.1146/annurev-fluid-010313-141424>
- [46] C. T. Sebens, “Forces on fields,” in *Studies in History and Philosophy of Science Part B: Studies in History and*

Philosophy of Modern Physics, 2018, pp. 1–11. <https://doi.org/10.1016/j.shpsb.2017.09.005>

- [47] Z. Wang, S. Wei, K. Bao, Y. Liu, S. Peng, and Q. Zhang, “Analysis of multiple failure behaviors of steering knuckle ball hinge of multi-axle heavy vehicle,” *Adv. Mech. Engr.*, vol. 13, no. 10, p. 168, 2021. <https://doi.org/10.1177/16878140211052287>
- [48] Y. C. Chen, H. H. Huang, and C. W. Weng, “Failure analysis of a re-design knuckle using topology optimization,” *Mech. Sci.*, vol. 10, no. 2, pp. 465–473, 2019. <https://doi.org/10.5194/ms-10-465-2019>